$$\frac{1}{T_g^s} = \frac{W}{T_g} + \frac{W^p}{T_g^p}$$

where W and W^p are the weight fractions of the pure polymer and pure plasticizer respectively, T_g, T_g^p and T_g^s are the glass transition temperatures of the pure polymer, pure plasticizer and plasticized sample respectively.

If the Fox equation applies, a plot of $1/T_g^s$ against W^p would be a straight line. However, when a plot of $1/T_g^s$ against percentage water content was constructed (*Figure 2*), it was found to be non-linear. It is therefore apparent that the water is not behaving just as a simple plasticizer in nylon-6. This more complex picture tends to support the mechanisms proposed by Puffr and Sebenda,[4] Kawasaki and Sekita[5], for the interaction of water with nylon-6.

The plot illustrated in *Figure 2* shows three distinct regions. The central portion of this graph shows little change in the T_g of the nylon-6 between 2.5 and 5% water content. Below 2.5% there is a rapid and almost linear increase in T_g with decreasing water content. Similarly about 5% there is an apparently linear, but less rapid

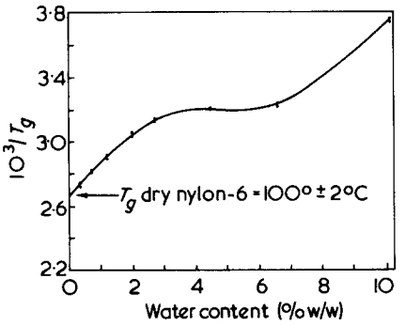

Figure 2 Fox plot for nylon-6

decrease in T_g with increasing water content. By extrapolation of the initial linear portion of this graph to zero water content, a value of 100° ± 2°C was obtained for the T_g of the dry nylon-6 granules.

The results show that the T_g of nylon-6 is markedly affected by water content and this is probably the explanation for the wide range of values quoted in the literature.

ACKNOWLEDGEMENTS

Thanks are expressed to Mr J. Hawke for helpful discussions.

REFERENCES

1 Def Stan 93-811, Annex B
2 Kaimin', I. F., Apinis, A. P. and Galvanowskii, A. Ya. *Polym. Sci. USSR* 1975, **17**, 46
3 Fox, T. G. *Bull. Am. Phys. Soc.* 1956, **1**, 123
4 Puffr, R. and Sebenda, J. *J. Polym. Sci. (C)* 1976, **16**, 79
5 Kawasaki, K. and Sekita, Y. *J. Polym. Sci. (A-2)* 1964, **2**, 2437
6 Wilusz, E. B. and Karasz, F. E. *Polym. Prepr.* 584, **16**
7 Rybnikar, F. *J. Polym. Sci.* 1958, **28**, 633
8 Forster, M. J. *Text. Res. J.* 1968, **38**, 474
9 Frosini, V. and Butta, E. *J. Polym. Sci. (Polym. Lett. Edn)* 1971, **9**, 253
10 Anton, A. *J. Appl. Polym. Sci.* 1968, **12**, 2117
11 Price, F. R., Pearce, E. M. and Fredericks, R. J. *J. Polym. Sci. (A-1)* 1970, **8**, 3533
12 Thomas, A. M. *Nature* 1957, **179**, 862
13 Doak, K. W. 1967, **45**, 14
14 Shibusawa, T. *J. Appl. Polym. Sci.* 1970, **14**, 1553
15 Takayanagi, M. *Rep. Prog. Polym. Phys. Japan* 1963, **6**, 121

Mosaic blocks in polymer crystals — the concept of paracrystallinity

J. Haase, R. Hosemann and H. Čačković

Fritz–Haber-Institut der Max–Planck-Gesellschaft, Teilinstitut für Strukturforschung, Berlin, Germany
(Received 30 December 1976; revised 14 March 1977)

Misunderstandings and misrepresentations in the literature[1,2] force us to clearly outline again the mosaic block concept in polymer crystals as it follows from numerous wide-angle (WAXS) and small-angle (SAXS) X-ray scattering studies.

The mosaic block concept is generally accepted for bulk polymers. However, on account of recent diffraction results from polymer single crystals it has been questioned 'as an intrinsic feature of polymer crystallization[2]. Therefore the present paper will be mainly concerned with diffraction measurements on single crystals. Two points will be stressed in the hope of clarifying the differences in explaining the diffraction results:

(1) X-ray line profile analysis proves that paracrystalline distortions define the limited sizes of the mosaic blocks called microparacrystals (*mPc*'s). Therefore the mosaic block concept does not invoke 'an intrinsic structural unit of a specific size and shape as a necessary attribute of polymer crystallization'.[2] For the same reason we do not believe the mosaic blocks in single crystal mats to be artefacts induced by sedimentation and drying.

(2) Our WAXS results on single crystal mats cannot be explained by chain obliquity, but positively prove the reality of *mPc*'s.

BLOCK SIZE AND DEFECT CONCENTRATION

Lamellae-shaped single crystals grown from dilute solution are seen in the electron microscope to extend laterally over many microns, whereas WAXS measurements on single crystal mats usually yield much smaller values for the coherently scattering domains. Consequently, it was assumed that a lamella consists of mosaic blocks. These are separated from each other laterally by twist-boundaries resulting in a slight rippling of moiré fringes[3].

The existence of paracrystalline distortions in polyethylene (PE) single crystal mats has been verified by analysing the linewidths of a number of wide angle reflections[4] and more recently by applying a Fourier method[5]. In the latter generally applicable analysis the Fourier coefficients A_n of the experimental line profiles of different orders of reflection are calculated. The logarithm of their ratio –

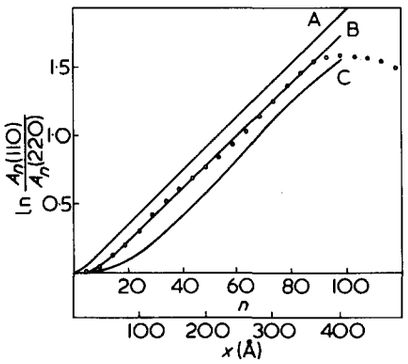

Figure 1 Plot of $\ln A_n(110)/A_n(220)$ vs. n for polyethylene single crystal mats (○). ——, represent theoretical fits with variable termination widths assuming paracrystalline lattice distortions. $A_n(hkl)$ is the Fourier-coefficient of the experimental hkl wide angle deflection. A, 20.5 β; B, 6.5 β; C, 3.5 β; $g_{110} = 1.6\%$; $\bar{D}_{110} = 560$ Å

plotted *versus* n – should give a straight line, if paracrystalline distortions are present. This is shown in *Figure 1* for PE single crystal mats. From the slope of the straight line the paracrystalline g-value is calculated which measures the amount of lattice distortions in the direction perpendicular to the reflecting net planes. To reach this result no assumption concerning the angle ϕ between the chain direction and the lamellar normal has been made.

The lateral dimensions of the *mPc*'s can vary considerably. In solution grown PE samples we found values ranging from about 200 Å up to more than 1200 Å [4].* Thus the mosiac block concept does not involve an intrinsic structural unit of a specific size. We believe and it has just been verified thermodynamically[8] that the size of the *mPc*'s is determined by the concentration of the built-in defects. For different polymers (solution and melt crystallized) as well as for all other microparacrystalline structures investigated till now the empirical relation:

$$\alpha^* = g\,(N)^{1/2};\ \alpha^* = \text{const} \simeq 0.1 \ldots 0.2 \qquad (1)$$

holds[9], where N is the number of net planes in a specific lattice direction of the crystal with paracrystalline distortions of magnitude g. If only a small number of defects is built into the lattice, N becomes large, i.e. the crystal can be highly regular. This is confirmed by recent electron diffraction measurements on PE single crystals showing lateral coherence over several 1000 Å [1] which again does not disagree with the mosaic block concept. The fact that the empirical constant α^* is the same for solution grown PE single crystals and melt crystallized PE shows that irrespective of the different morphologies the same mechanism works that couples the block size to the defects concentration. Therefore, we do not believe the mosaic blocks to be artefacts in polymer single crystal mats. By sedimentation and drying the lamellae certainly bend, collapse and rupture. However, there is a high probability that the rupture will take place at the twist-boundaries, thereby introducing no artefacts. Hence the existence of mosaic blocks of distortion-dependent size seems to be a general feature of polymer crystals.

CHAIN OBLIQUITY AND BLOCK SIZE

It is assumed[2] that the broadening of the equatorial WAXS reflections of single crystals in suspension† – the broadening effect of the lattice distortions being separated – is not due to the finite lateral block size D according to the well-known relation:

$$\delta b = 1/D \qquad (2)$$

but instead of this could be explained by infinitely large and slightly misoriented lamellae of thickness T with chains tilted by an angle φ around an axis A parallel to the lamellar surface. If α is the angle between an equatorial net plane ($hk0$) and the A-axis, then the linewidth of a $hk0$-reflection of this assembly is given by:

$$\delta b = \sin\varphi \sin\alpha/T \qquad (3)$$

In ref 2 only the case with $\alpha = 90°$ is discussed.

Combined SAXS and WAXS analysis proved that in our single crystal mats the chains were tilted by an angle $\varphi = 22°$ around the crystallographic b-axis‡. In *Figure 2* the intensity distribution along the 020, 110 and 200-reflection arcs of a flat camera diagram as function of the angle β between the measuring position and the equator is plotted. Obviously the 020-reflection is practically not splitted, whereas the 200 shows a distinct splitting. Assuming for all intensity distributions the experimental 020-profile, the curves for the 200- and 110-reflections can be resolved into two components with splitting angles of $\beta = 22°$ and $\beta = 12°$, respectively. The arrows in *Figure 2* indicate the positions of the maxima, if a chain tilt of $\phi = 22°$ around the b-axis is assumed.

As a further result the δb-values for the 200- and 020-reflections obtained with a high resolution Guinier-camera are of the same order of magnitude. If the lamellae were infinitely large, the 020-reflection with $\alpha = 0$ should be infinitely sharp according to equation (3). This, clearly, is not the case. The 020 width, therefore, is given by equation (2); the measured size in [010] direction is a true block size.

The same must hold for all other measured lateral sizes. Although the width of the 200-reflection could be explained by equation (3), annealing effects – where the crystal thickness nearly doubles and the lateral sizes remain practically constant[11] – show that δb of the equatorial reflections does not obey equation (3). Moreover, the evaluation of continuous SAXS reveals domains of higher electron density which agree in size with the coherently scattering domains measured by WAXS on the same sample[3]. This shows that the broadening of the equatorial WAXS reflections – the broadening effect of the lattice distortions being separated – is mainly given by the

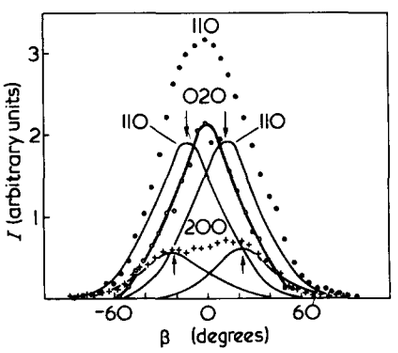

Figure 2 Maximum intensity along the 020 (○), 110 (●) and 200 (+) reflection arcs of polyethylene single crystal mats vs. the angle β between the measuring position and the equator. The 110 and 200 intensity distributions may be resolved as two overlapping components (presuming the same intensity profile as the 020) with splitting angles of 12° and 22°, respectively

* Such large values can be found also in melt crystallized material, for instance in extended chain PE[6] and in doubly oriented PE[7].

† Detailed results are not yet published.

‡ Tilts around the b-axis were also observed with stretched branched PE[10] and in doubly oriented PE[7].

lateral size of the *mPc*'s.

Another striking example for the existence of mosaic blocks in single crystal mats is found in the degradation experiments with fuming HNO_3 [4]. Within experimental error the lamellar thickness remains constant during the degradation. If chain obliquity and equation (3) would really play a dominant role the lateral sizes also should stay constant. This again is not the case. The lateral sizes of the *mPc*'s are drastically diminished as the acid interpenetrates the mosaic blocks from the grain-boundaries.

REFERENCES

1 Thomas, E. L., Sass, S. L. and Kramer, E. J. *J. Polym. Sci.* 1974, **12**, 1015
2 Harrison, I. R., Keller, A., Sadler, D. M. and Thomas, E. L. *Polymer* 1976, **17**, 736
3 Hosemann, R., Wilke, W. and Baltá-Calleja, F. J. *Acta Crystallogr.* 1966, **21**, 118
4 Schönfeld, A., Wilke, W., Höhne, G. and Hosemann, R. *Kolloid Z. Z. Polym.* 1972, **250**, 110
5 Vogel, W., Haase, J. and Hosemann, R. *Z. Naturforsch. (A)* 1974, **29**, 1152
6 Schönfeld, A. and Wilke, W. *Kolloid Z. Z. Polym.* 1972, **250**, 496
7 Kaji, K., Mochizuki, T. and Hosemann, R. in press
8 Lindenmeyer, P. H., Beumer, H. and Hosemann, R. in press
9 Hosemann, R. *J. Polym. Sci. Polym. Symp.* 1975, **53**, 265
10 Loboda-Čačković, J., Čačković, H. and Hosemann, R. *J. Polym. Sci. Polym. Symp.* 1973, **42**, 577
11 Wilke, W., Vogel, W. and Hosemann, R. *Kolloid Z. Z. Polym.* 1974, **237**, 317

Plastic fracture of polystyrene

K. Smith and R. N. Haward,*

Centre for Materials Science, University of Birmingham, Birmingham B15 2TT, UK

(Received 7 March 1977)

INTRODUCTION

Previous work has shown that a number of common thermoplastic materials undergo ductile fracture in the manner first described by Cornes and Haward for PVC.[1] These include cellulose acetate[2], polycarbonate, poly(ether sulphone) and poly(methyl methacrylate)[3], the last three at elevated temperatures. Ductile fracture in these cases results from the growth by tearing of one or more diamond shaped cavities generally initiated at the surface of yielded material from crazes if present or, generally, from other surface defects. A fast running crack then develops as the stress on the remaining cross-section reaches some critical value resulting in the formation of characteristic fracture surfaces. Cornes *et al.*[4], have referred to this process as 'plastic fracture' so as to distinguish it from a conventional 'brittle' type craze to crack mechanism.

Recent work with polystyrene has indicated that under suitable conditions of testing this material, like those cited above, will also show plastic fracture.

EXPERIMENTAL

The material used was a pure extruded sheet supplied by the Shell Chemical Company and having a glass transition temperature of 100°C. Standard dumbbell test-pieces were prepared and tested using a floor mounted Instron equipped with an environmental chamber for work at elevated temperatures. Electron microscopy was carried out using a Cambridge Instruments S4 'stereoscan' using an accelerating voltage of not more than 10 kV. All specimens were prepared for observation by covering with an ~100 Å gold film to prevent both charging up and damage under the applied electron beam.

RESULTS

Tensile behaviour

At strain rates of less than 2.5×10^{-4} sec^{-1} and temperatures above 80°C necking and post yield deformation occurred. At temperatures above 90°–95°C no distinct yield point was evident and the material was considered to be no longer in the glassy state.

Scanning electron microscopy

Figure 1 shows a number of surface

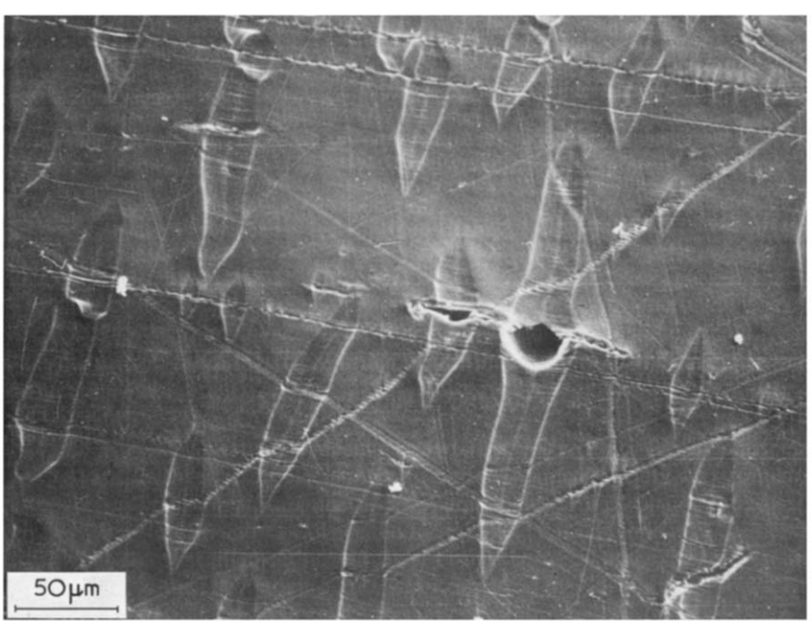

Figure 1 Scanning electron micrograph showing widened crazes in bulk yielded polystyrene

* Present address: BXL Cascelloid Division, Leicester, UK.